Theoretical studies on the electron-impact excitation of neutral magnesium

R. E. H. Clark, G. Csanak, and J. Abdallah, Jr.
Los Alamos National Laboratory, Los Alamos, New Mexico 87545
(Received 17 December 1990; revised manuscript received 2 April 1991)

We used the distorted-wave approximation (DWA) and first-order many-body theory (FOMBT) for the calculation of integral cross sections (ICS's), differential cross sections (DCS's), and electron-impact coherence parameters (EICP's) for electron-impact excitation of neutral magnesium for several transitions. In the case of $3\,^1P$ excitation, we studied the basis-set dependence of the ICS's, DCS's, and EICP's, we investigated the effect of unitarization on these quantities, and we compared the DWA with FOMBT. We also studied the principal-quantum-number dependence of the EICP's for $n\,^1P$ ($n=3,4,5,6$) excitation.

I. INTRODUCTION

The electron-impact excitation of magnesium is of considerable scientific interest. The main reason for this is that Mg is a relatively small atom with a ^1S ground state, and both the ground and excited states of Mg can be well described within the LS-coupling formalism [1]. On the other hand, Mg as a target in electron-impact processes shows significant differences compared to He, a much-studied target in theoretical and experimental studies of electronic collisions [2]. While the ground state of Mg is also a closed-shell ^1S state, it shows strong electron-correlation effects [3] and the lowest-lying optically allowed (resonance) state of magnesium, the $3\,^1P$ state, is strongly coupled to the $3\,^1S$ ground state (with an optical f value of ~ 1.8) [3]. Therefore, from the theoretical standpoint, it is interesting to investigate the influences of these features on the various types of information obtainable from electron-scattering experiments.

Recently, new experimental data and results from theoretical calculations have been reported for e-Mg scattering. Brunger *et al.* [4] reported differential-cross-section (DCS) data for the electron-impact excitation of the $3\,^1P$ state of Mg at 10-, 20-, and 40-eV incident electron energies and Brunger *et al.* [5] reported results for electron-impact coherence parameters (EICP's) from electron-photon coincidence experiments for the 3^1P state of Mg at 20- and 40-eV incident electron energies. On the theoretical side, there was also considerable activity. Mitroy and McCarthy [6] reported DCS, EICP, and integral-cross-section (ICS) results for elastic scattering and for the excitation of the $3\,^1P$ and $3\,^1D$ states of Mg at 10-, 20-, 40-, and 100-eV incident electron energies from a five-state close-coupling (5CC) calculation, and McCarthy, Ratnavelu, and Zhou [7] reported DCS and ICS results at 10-, 20-, and 40-eV incident electron energies for the excitation of the $3\,^1P$ and $3\,^3P$ states from a six-state optical-potential CC (6CCO) calculation. Meneses, Pagan, and Machado [8] reported DCS and EICP results for six incident electron energies in the 10 eV $\leq E \leq$ 100 eV energy range for $3\,^1P$ and $3\,^3P$ excitation. These latter experimental and theoretical works discuss in detail earlier experimental and theoretical works to which the reader is referred for details.

The purpose of the present paper is to report results from a series of distorted-wave approximation (DWA) type of calculations for ICS's, DCS's, and some EICP's for various electron-impact-induced transitions in Mg. One of our purposes was to study theoretically the importance of some of the features of Mg on these quantities that we mentioned earlier. These features include the influence of target-correlation effects in the initial and final states of the transition considered as well as the significance of the strong optical coupling between the $3\,^1S$ and $3\,^1P$ states of Mg. This latter effect can be studied by comparing DWA results with results from unitarized DWA (UDWA) [9]. We also compare sightly different versions of DWA such as first-order many-body theory (FOMBT) [10] with the conventional DWA. In the case of He target, such a study was undertaken by Madison and Shelton [11]. We also show a study for the principal-quantum-number dependence of the transferred angular momentum as was performed for helium [12].

II. METHOD OF CALCULATION

Our method of calculation was described earlier in detail by Clark *et al.* [13,14] and will be only briefly summarized here. The calculations were performed by the subsequent running of three computer codes named CATS, ACE, and TAPS. Atomic structure calculations are performed with the CATS code [15], a modified version of Cowan's atomic structure codes [16–19]. The atomic-structure calculation is initiated by a single-configuration Hartree-Fock calculation for the radial wave functions of each configuration. Mixing among all configurations and LS terms with the same total angular momentum J and parity is then obtained through perturbation theory.

The electron-collision calculations are performed using the ACE code [20]. This code reads in data from the atomic-structure file and calculates electron-impact-collision strengths using a variety of options. The collision strengths can be converted to cross sections using the TAPS code. The ACE code uses the DWA of Mann

[21] or FOMBT [10]. The only difference between the DWA and FOMBT calculations is that in the former case (i.e., for DWA), we calculate the continuum wave function in the potential of the initial and final configurations for the incident and scattered electrons, respectively, whereas in the latter case (i.e., for FOMBT), the same potential (that of the initial configuration) is used for both continuum electrons. The reactance matrix elements are first calculated between LS terms as in Mann's approach [21]. Unitarization of the reactance matrix is normally carried out; however, unitarization can be ignored for comparison purposes. Recoupling is then done using the pair-coupling scheme of Saraph [22]. Inclusion of configuration-interaction and intermediate-coupling mixing is obtained as by Clark [23].

If desired, the user can request DCS's from the ACE code. The ACE code then uses the reactance matrix along with continuum wave-function phases to calculate the scattering amplitudes using the recoupling scheme of Inal and Dubau [24]. The scattering amplitudes are stored on a data file and can be used to calculate DCS's and EICP's via the TAPS code [25].

In the calculation of the ICS's, denoted here by Q, in order to speed up convergence, the first-order Born approximation value Q^{PWB} is added (in closed form) and subtracted (in partial wave form) according to the formula

$$Q = Q^{\mathrm{PWB}} + \sum_{l=0}^{l_{\max}} (Q_l^{\mathrm{DWA}} - Q_l^{\mathrm{PWB}}) ,$$

where Q_l^{DWA} is the partial-wave DWA integral cross section, and Q_l^{PWB} is the first-order Born approximation partial-wave integral cross section. Thus the number of distorted partial waves ($l_{\max}$) to be calculated is usually small. In the calculations reported here, convergence was achieved by about $l_{\max} \approx 35-50$ distorted partial waves.

In the calculation of the DCS's and EICP's, the above procedure (of adding and subtracting the Born approximation) is not used, and typically $l_{\max} = 250$ partial waves are used, except in few cases (mentioned in the figure captions) where we had to use up to $l_{\max} = 395$ partial waves, which is the current upper limit in the computer program.

III. NUMERICAL RESULTS AND DISCUSSION

A. Integral cross-section (ICS) results

We performed numerical calculations for the transitions shown in our Table I, where we also show the calculated and observed excitation energies from Radzig and Smirnov [26]. We show in Tables II–V and Figs. 1–4 the results obtained for the ICS's for the transitions studied, and we compare our results with selected other theoretical results and with experimental data available. All present results shown in Figs. 1–4 were obtained via unitarization. In the case of the $3\,^1S \rightarrow 3\,^1P$ electron-impact-induced transition, Table II shows that unitarization has a strong effect on the ICS at low energies decreasing the nonunitarized value by about 30% at 10-eV incident electron energy, while its effect at higher ener-

TABLE I. Calculated (ΔE_{calc}) and observed (ΔE_{obs}) excitation energies of the transitions shown.

Transition	ΔE_{calc}	ΔE_{obs} [a]
$3\,^1S-3\,^3P$	2.5383	2.7141
$3\,^1S-3\,^1P$	4.3847	4.3458
$3\,^1S-3\,^1D$	5.8414	5.7533
$3\,^1S-4\,^1S$	5.4304	5.3938

[a]From Radzig and Smirnov [26].

TABLE II. Comparison of theoretical results for the integrated cross section (in πa_0^2 units) for the electron-impact excitation of the $3\,^1P$ state of magnesium.

	10 eV	20 eV	40 eV	100 eV
DWA[a]	30.17	26.61	19.28	10.76
FOMBT[b]	28.74	26.73	19.43	10.84
UDWA[c]	19.81	20.90	16.90	10.23
UFOMBT[d]	19.13	20.85	17.00	10.30
FBA[e]	36.02	29.17	20.08	10.92
CC5[f]	16.90	18.60	15.50	9.5
6CC[g]	15.76	18.50	15.79	
6CCO[h]	15.25	14.81	14.21	
5UB[i]	15.6	18.9	15.8	9.5
FBA[j]	32.6	26.8	18.7	10.2
FBA[k]	41.97		21.81	11.60

[a]Present DWA results (with configuration mixing).
[b]Present FOMBT results (with configuration mixing).
[c]Present unitarized DWA results (with configuration mixing).
[d]Present unitarized FOMBT results (with configuration mixing).
[e]Present first-order Born approximation results (with configuration mixing).
[f]Five-state coupled-channels-calculation results of Mitroy and McCarthy (Ref. [6]).
[g]Six-state coupled-channels-calculation results of McCarthy, Ratnavelu, and Zhou (Ref. [7]).
[h]Six-state optical-potential-calculation results of McCarthy, Ratnavelu, and Zhou (Ref. [7]).
[i]Unitarized Born approximation to CC5 (5UB) results of McCarthy, Ratnavelu, and Zhou (Ref. [7]).
[j]First-order Born approximation results of McCarthy, Ratnavelu, and Zhou (Ref. [7]).
[k]First-order Born approximation results of Robb (Ref. [3]).

TABLE III. Comparison of theoretical results for the integrated cross section (in πa_0^2 units) for electron-impact excitation of the $3\,^3P$ state of magnesium. Notation is the same as in Table II.

	10 eV	20 eV	40 eV
DWA	6.11	0.762	0.085
FOMBT	6.96	0.831	0.088
UDWA	5.34	0.749	0.084
UFOMBT	5.84	0.814	0.088
6CC	4.13	0.76	0.063
6CCO	4.31	0.69	0.093

TABLE IV. Comparison of theoretical results for the integrated cross section (in πa_0^2 units) for electron-impact excitation of the $3\,^1D$ state of magnesium. Notation is the same as in Table II.

	10 eV	20 eV	40 eV	100 eV
DWA	1.72	1.84	1.21	0.554
FOMBT	1.30	1.72	1.19	0.546
UDWA	1.70	1.82	1.21	0.552
UFOMBT	1.28	1.71	1.18	0.544
FBA	3.22	2.28	1.29	0.554
5CC	1.92	1.69	1.17	0.585

TABLE V. Comparison of theoretical results for the integrated cross section (in πa_0^2 units) for electron-impact excitation of the $4\,^1S$ state of magnesium. Notation is the same as in Table II.

	10 eV	20 eV	40 eV	100 eV
DWA	5.12	2.72	1.37	0.54
FOMBT	2.55	2.13	1.24	0.52
UDWA	3.68	2.11	1.14	0.48
UFOMBT	1.84	1.50	0.88	0.37
FBA	2.95	2.07	1.18	0.50
5CC	1.16	0.826	0.649	0.255

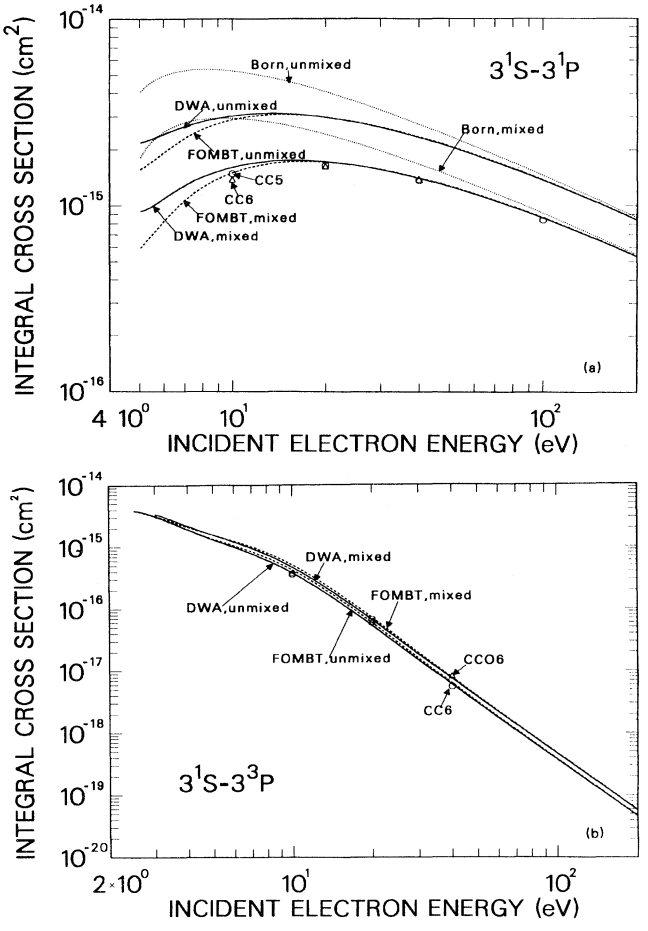

FIG. 1. Comparison of present DWA and FOMBT results (both unitarized) for the integral cross section using single-configuration target states (unmixed) and configuration-mixed target states (mixed) with the five-state close-coupling (5CC) results of Mitroy and McCarthy (Ref. [6]), with the six-state close-coupling (6CC) results and with the six-state optical potential close-coupling (6CCO) results of McCarthy, Ratnavelu, and Zhou (Ref. [7]) for (a) the $3\,^1S \rightarrow 3\,^1P$ electron-impact-induced transition and (b) the $3\,^1S \rightarrow 3\,^3P$ electron-impact-induced transition.

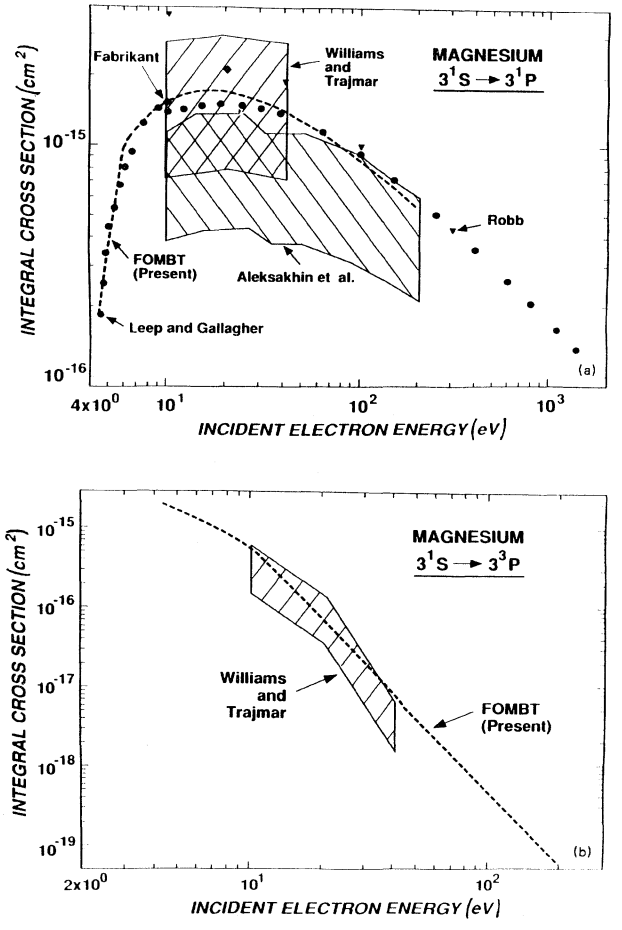

FIG. 2. (a) Comparison of the present unitarized FOMBT results for the integral cross section with the experimental results of Ref. [29] (labeled as Aleksakhin *et al.*), with that of Ref. [30] (labeled as Leep and Gallagher), and with that of Ref. [28] (labeled as Williams and Trajmar), as well as with the theoretical two-state close-coupling results of Ref. [31] (labeled as Fabrikant) and with the first-order Born approximation results of Ref. [3] (labeled as Robb) for the electron-impact-induced $3\,^1S \rightarrow 3\,^1P$ transition of magnesium. (b) Comparison of the present unitarized FOMBT results for the integral cross section with the experimental results of Ref. [28] (labeled as Williams and Trajmar) for the electron-impact-induced $3\,^1S \rightarrow 3\,^3P$ transition of magnesium.

gies is small. This can be understood since, as we mentioned earlier, the $3\,^1S \rightarrow 3\,^1P$ is strongly coupled, and the weak-coupling conditions for the applicability of DWA is not satisfied, and, under those conditions, unitarization is essential and it changes results significantly. At 100-eV incident electron energy, the UDWA and unitarized FOMBT (UFOMBT) results essentially agree with the 5CC results if one considers the fact that the present first-order Born approximation (FBA) results are higher than those of McCarthy, Ratnavelu, and Zhou [7] due to the use of configuration-mixed-target wave functions. Robb's accurate FBA results [3] are even higher than ours.

In the case of the $3\,^1S \rightarrow 3\,^3P$ electron-impact-induced transition, Table III shows that unitarization has less effect in this case than in the $3\,^1S \rightarrow 3\,^1P$ case, which is understandable since this is a pure exchange transition and thus it is weak, and, consequently, the conditions for weak-coupling conditions hold. Table III also shows that the UDWA and UFOMBT results are still considerably higher than the 6CC and 6CCO results at 10 eV. In the case of this transition, the ICS results do not reveal much about the accuracy of approximation, which can be judged better by comparing DCS results. FOMBT results for the DCS were presented by Meneses, Pagan, and Machado [8], and their comparison with 6CCO results was discussed by Mitroy and McCarthy [6]; therefore we shall not go into further detail here.

In the case of the $3\,^1S \rightarrow 3\,^1D$ electron-impact-induced transition, Table IV shows that the present DWA and FOMBT results for the ICS's essentially agree with the 5CC results of Mitroy and McCarthy [6], and, again, unitarization does not effect those results significantly since weak-coupling conditions hold here, also. The applicability of the DWA for $S \rightarrow D$ type of transitions is an interesting problem to which we plan to return in a future paper.

Figures 1 and 3 show ICS's obtained using DWA versus FOMBT and unmixed or mixed wave functions for the target states. Mixing is among all terms of all configurations with the same J and parity. For parity-

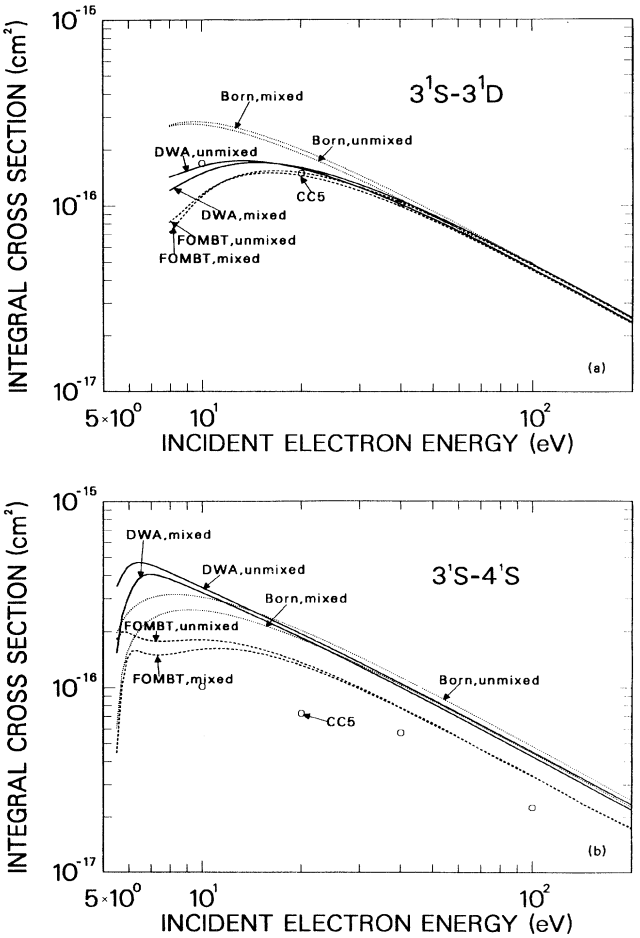

FIG. 3. Same as Fig. 1 except for (a) the $3\,^1S \rightarrow 3\,^1D$ transition, and (b) the $3\,^1S \rightarrow 4\,^1S$ transition.

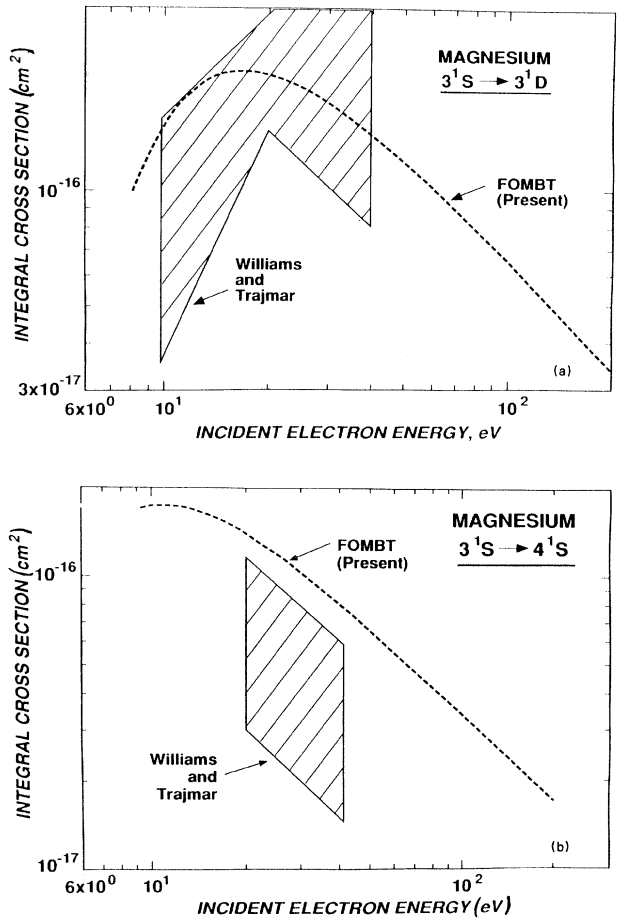

FIG. 4. Comparison of the present unitarized FOMBT results for the integral cross section with the experimental results of Ref. [28] (labeled as Williams and Trajmar) for (a) the electron-impact-induced $3\,^1S \rightarrow 3\,^1D$ transition, and (b) the $3\,^1S \rightarrow 4\,^1S$ transition.

changing transitions, the ground-state $3s^2$ configuration includes mixing with the $3p^2$ configuration. The excited states include the $3s3p$, $3s4p$, $3p4s$, and $3p3d$ configurations. For parity-conserving transitions, the basis set included the $3s^2$, $3p^2$, $3d^2$, $3p4p$, and $3s4s$ configurations. Figures 1 and 3 show strong configuration-mixing effects on the ICS's. In the case of $3\,^1S \rightarrow 3\,^1P$ excitation, configuration mixing significantly lowers the ICS, whereas in the case of $3\,^1S \rightarrow 3\,^1D$ transition, it increases. As Fig. 1(a) shows, configuration mixing decreases the ICS to bring it into reasonably good agreement with the 5CC and 6CC results. The agreement of the unitarized FOMBT results [shown in Fig. 1(b)] with experiment is quite good; however, as mentioned earlier, the experimental errors are quite large due to the high-temperature nature of the Mg target. One can also note that DWA and FOMBT give practically identical results for the ICS's studied for $E > 30$ eV incident electron energies, and for the excitation of the spin-forbidden $3\,^3P$ state, the agreement extends to practically the whole energy range except for the near-threshold region. Figures 2 and 4 compare our (unitarized) FOMBT results to several experimental results for the ICS available in the literature. The shaded regions in these figures represent the range of experimental uncertainty in the cross section. One can see that agreement with the experimental ICS data is quite good except for the $3\,^1S \rightarrow 4\,^1S$ transition where the theoretical results are somewhat high. We note here that to obtain accurate experimental ICS data for Mg target is quite difficult, Mg being a high-temperature species and the estimation of the number of Mg atoms in the scattering chamber is a difficult task. Therefore our theoretical results for a variety of transitions might be useful for normalizing the experimental data.

B. Differential cross-section (DCS) results

Figure 5 shows our DCS results for the $3\,^1S \rightarrow 3\,^1P$ excitation for $E = 10$ and 40 eV incident electron energies using three different basis sets. One can immediately see that the inclusion of the $3p^2$ configuration into the ground-state wave function (i.e., ground-state correlation effect) is important at both energies; however, the inclusion of the $3p3d$ configuration (i.e., the correlation effect in the $3\,^1P$ state) has practically no influence on our results. One sees from Fig. 5 that, although the DCS

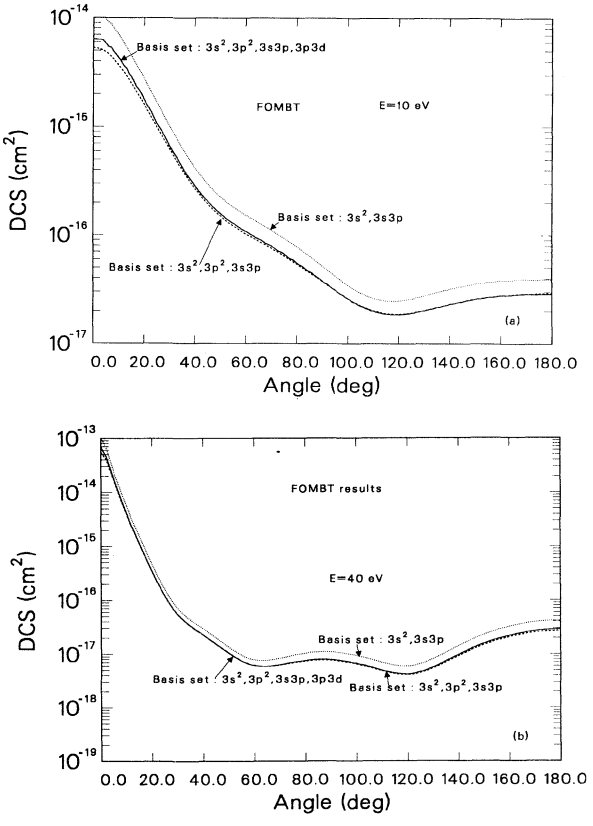

FIG. 5. Basis-set dependence of the differential cross section (DCS) calculated by FOMBT for the excitation of $3\,^1P$ state of Mg at (a) $E = 10$ eV incident electron energy and (b) $E = 40$ eV incident electron energy. (Present calculations included 395 partial waves.)

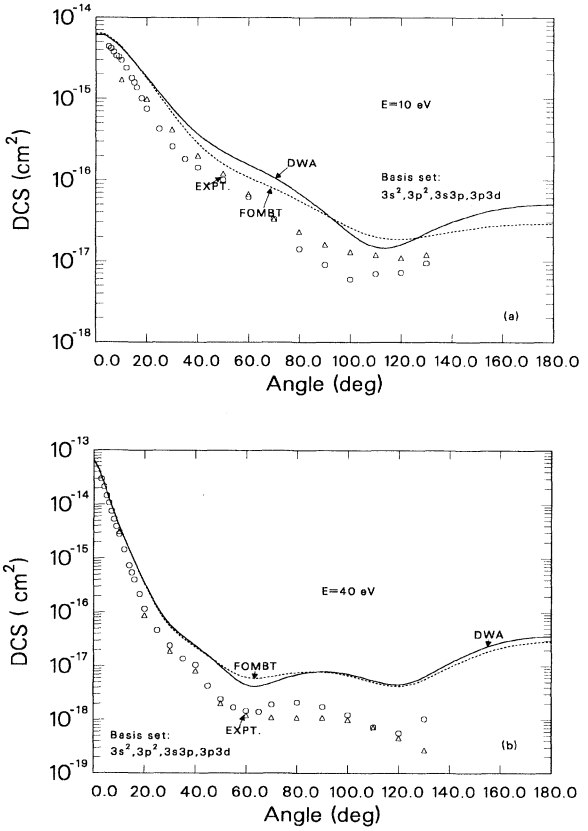

FIG. 6. FOMBT vs DWA results for the DCS for the $3\,^1P$ excitation of Mg. Experimental results shown are those of Williams and Trajmar (Ref. [28]), triangles; and Brunger *et al.* (Ref. [4]), octagons at (a) $E = 10$ eV incident electron energy and (b) $E = 40$ eV incident electron energy.

changes significantly with the inclusion of the $3p^2$ configuration, the resulting DCS curve is nearly parallel to the DCS curve without the $3p^2$. In fact, the inclusion of the $3p^2$ configuration would result in a simple multiplication by a real number of at least the direct T-matrix element, as noted by Meneses, Pagan, and Machado [8], if (i) the ground-state $3s$ and $3p$ orbitals were the same as the excited state $3s$ and $3p$ orbitals; and (ii) all continuum orbitals and phase shifts were the same in the $(3s^2,3p^2,3s3p)$ basis-set calculation as in the $(3s^2,3s3p)$ basis-set calculation. These conditions were satisfied in the calculation of Meneses, Pagan, and Machado. Even though these conditions are not rigorously satisfied for our calculation, they are satisfied to a good approximation. This can be seen from Fig. 5 where the $(3s^2,3s3p)$ basis-set curve runs parallel to the $(3s^2,3p^2,3s3p)$ basis-set curve everywhere except for small angles showing that the above-mentioned small deviations give an accumulated effect for small angles.

Figure 6 compares our FOMBT and DWA results for the $3\,^1S\rightarrow 3\,^1P$ excitation DCS at $E=10$ and 40 eV incident electron energies. Some experimental data are also shown. It can be seen clearly that at the lower energy studied, there are considerable differences in the FOMBT and DWA results for $\theta>30°$ scattering angles, but these differences practically disappear at $E=40$ eV incident electron energy.

Figure 7 shows the effect of unitarization on the DCS at $E=10$ and 40 eV incident electron energies. At both energies, unitarization improves agreement with experiment; however, while the improvement at the lower energy is quite dramatic, at the higher energy there remains a strong deviation from the experiment for $\theta>15°$ scattering angle.

C. Electron-impact coherence parameter (EICP) results

Figure 8 shows our results for the λ and χ EICP's [27] in the FOMBT for the $3\,^1S\rightarrow 3\,^1P$ excitation using different basis sets. It can be seen that the inclusion of correlation into the ground- and excited-state wave functions has practically no effect on the EICP's. Even the inclusion of ground-state correlation shows no perceptible influence. This is quite different from what we have seen in the case of our DCS studies. However, it can be understood if we remember our earlier comments, and if we recall the definition of the λ and χ parameters [8], given as

$$\lambda=\frac{\sigma_0}{\sigma_0+2\sigma_1},\quad \chi=\arg T_1-\arg T_0\equiv\arg(T_1/T_0)\ ,$$

where T_M is the electron-scattering matrix and σ_M is the

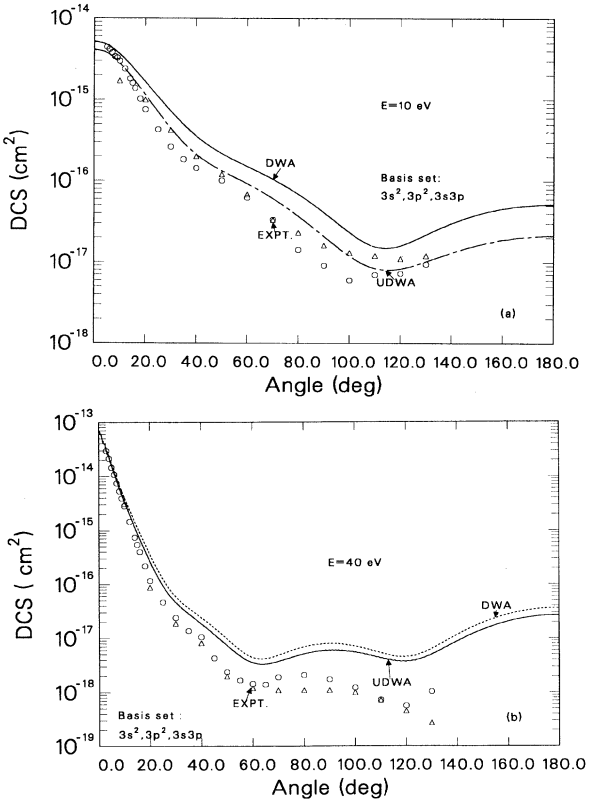

FIG. 7. DWA vs UDWA results for the DCS for the $3\,^1P$ excitation of Mg. Experimental results shown are those of Williams and Trajmar (Ref. [28]), triangles; and Brunger *et al.* (Ref. [4]), octagons at (a) $E=10$ eV incident electron energy and (b) $E=40$ eV incident electron energy.

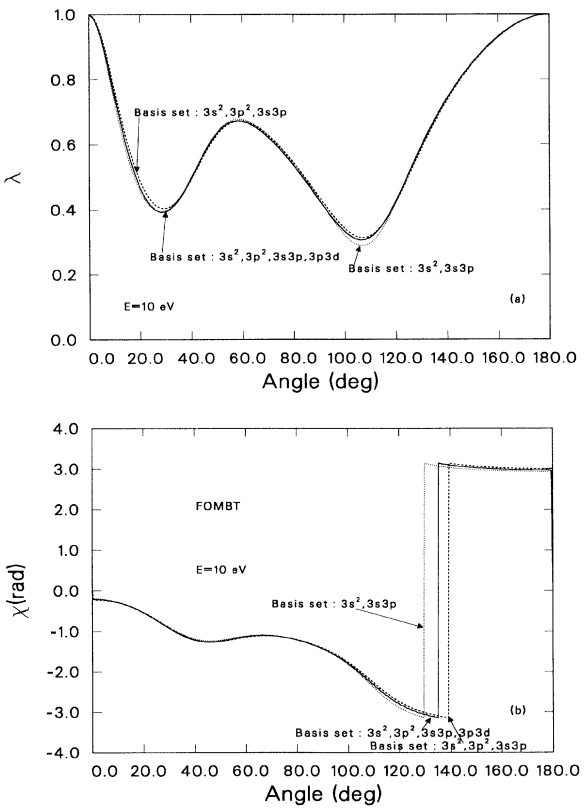

FIG. 8. Basis-set independence of (a) λ and (b) χ EICP's for Mg $3\,^1S\rightarrow 3\,^1P$ excitation at $E=10$ eV incident electron energy.

electron-impact-excitation differential cross section (proportional to $|T_M|^2$), respectively, for the excitation of the M sublevel of the $3\,^1P$ level. λ and χ are relative quantities, i.e., they depend only on the T_1/T_0 ratio. If the inclusion of the $3p^2$ configuration into our basis set results in a multiplication (by a real number) of T_1 and T_0, then this factor does not influence λ and χ. If this multiplier depends on the scattering angle, then λ and χ still remain unchanged if T_1 and T_0 are affected the same way, which appears to be the case for small angles.

Figure 9 shows our results for the λ and χ EICP's using DWA and UDWA at $E=10$ eV incident electron energy. One can see that unitarization has a perceptible but small effect on these parameters. This, again, can be understood by an inspection of Fig. 7, which shows that unitarization is essentially equivalent in this case to the introduction of a scale factor, which cancels again in the calculation of EICP's.

Figures 10–13 show our theoretical results for the P_1 and P_2 Stokes parameters and for $\langle L_Y\rangle = -P_3$, the transferred angular momentum (in atomic units) perpendicular to the collision frame, for $E=40$ eV incident energy electrons. Our theoretical results are compared to the experimental results of Brunger *et al.* [5]. In the case of P_2, DWA and UDWA show superb agreement with the experiment, the agreement with the experiment for $\langle L_Y\rangle$ is reasonable, while for P_1 at $\theta=15°$ and 20° scattering

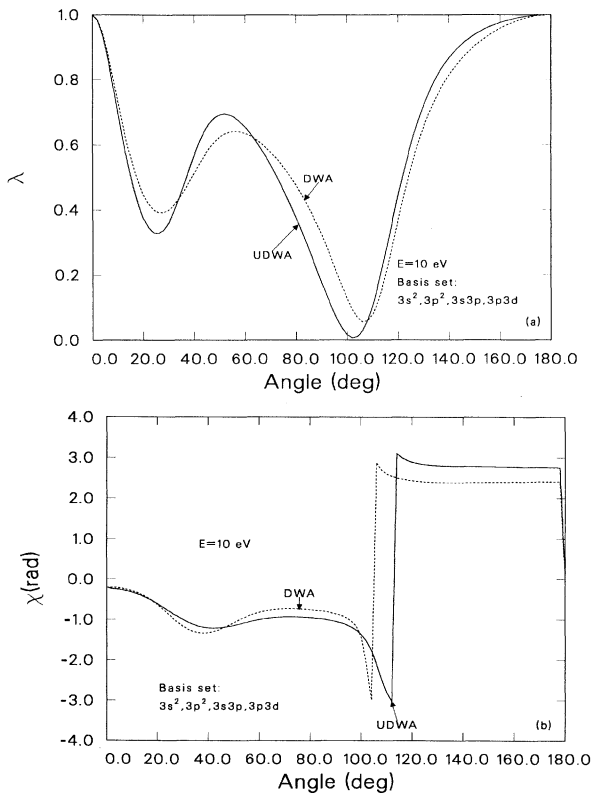

FIG. 9. DWA vs UDWA results for the (a) λ and (b) χ EICP's at $E=10$ eV incident electron energy.

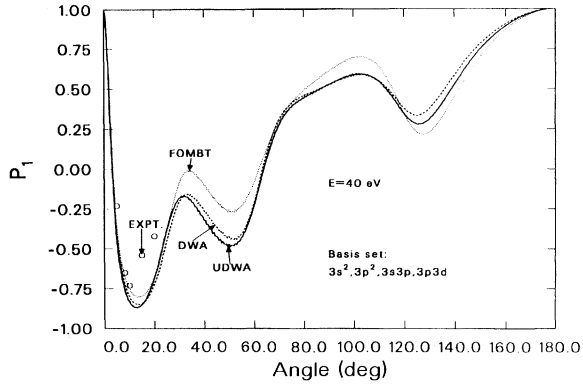

FIG. 10. FOMBT, DWA, and UDWA results for the P_1 Stokes parameter for $3\,^1P$ excitation of Mg with $E=40$ eV incident energy electrons.

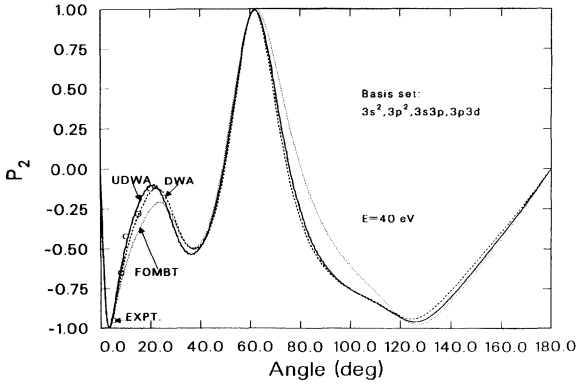

FIG. 11. Same as Fig. 10 except for the P_2 Stokes parameter.

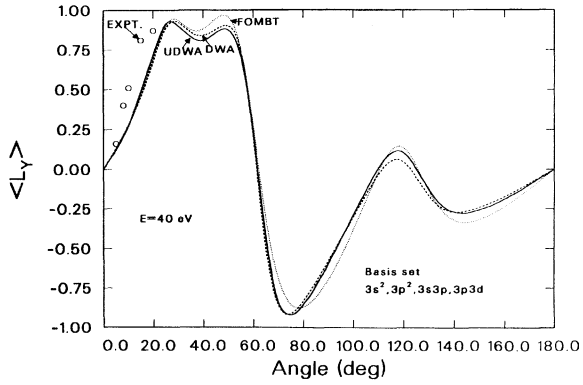

FIG. 12. Same as Fig. 10 except for the average transferred angular momentum $\langle L_Y\rangle = -P_3$ (in atomic units) where P_3 is the third Stokes parameter.

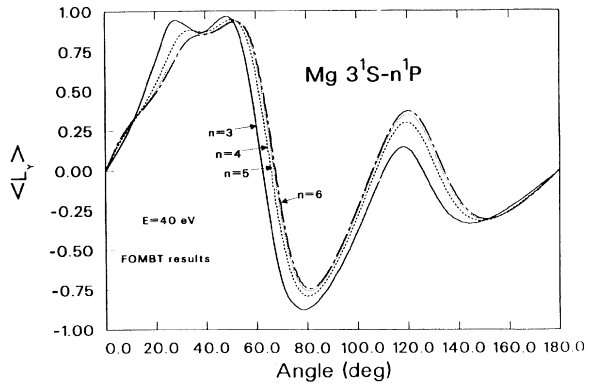

FIG. 13. Principal quantum number dependence of the transferred angular momentum $\langle L_Y \rangle$ (in atomic units) for $n=3,4,5,6$. (Present calculations included 395 partial waves.)

angles, our results differ significantly from the experimental data.

Figure 13 shows $\langle L_Y \rangle$ for the excitation of $n\,^1P$ ($n=3,4,5,6$) states of Mg. As found [12] for He, $\langle L_Y \rangle$ calculated from FOMBT is practically independent from the principal quantum number n. This can be understood, as in the case of He [12], on the basis of quantum-defect-theory type of arguments. The essential n independence found for Mg is quite remarkable since Mg $3\,^1S$ is a very extended state, and the $3s$ orbital overlaps with the np ($n=3,4,\ldots$) orbitals for larger distances than the analogous orbitals for helium.

IV. SUMMARY AND CONCLUSIONS

We have performed DWA-type calculations for a variety of electron-impact-induced transitions in magnesium. We studied the influence of target-state wave functions used in the calculation and unitarization on our results, and we compared our DWA results with FOMBT results.

We found that the inclusion of target correlation in the ground-state wave function strongly influences the ICS and DCS results, especially at low energies, but has little influence in the EICP's. We also found that unitarization has a strong effect on the ICS and DCS results, but has only a weak effect on the EICP's. We found that essential n independence of the EICP's for $3\,^1S \rightarrow n\,^1P$ ($n=3,4,5,\ldots$) transitions at $E=40$ eV incident electron energy holds for Mg, also, as it was valid for $1\,^1S \rightarrow n\,^1P$ ($n=2,3,\ldots$) transitions in He.

ACKNOWLEDGMENTS

The authors acknowledge the financial support of the U.S. Department of Energy and the National Science Foundation, Office of International Programs. They thank R. D. Cowan, J. B. Mann, and A. L. Merts for their cooperation in the development of the atomic physics codes. They thank D. C. Cartwright for his support and interest in this work.

[1] For spectroscopic studies on Mg, see, e.g., Y.-K. Kim and P. S. Bagus, J. Phys. B **5**, L193 (1972), and references therein.

[2] For reviews on electron scattering from atoms, see, e.g., B. H. Bransden and M. R. C. McDowell, Phys. Rep. **30**, 207 (1977); **46**, 249 (1978); I. I. Farbrikant, O. B. Shpenik, A. V. Snegursky, and A. N. Zavilopulo, *ibid.* **159**, 1 (1988).

[3] For the importance of electron-correlation effects in the ground and resonance state of Mg for the Born cross section, see W. D. Robb, J. Phys. B **7**, 1006 (1974).

[4] M. J. Brunger, J. L. Riley, R. E. Scholten, and P. J. O. Teubner, J. Phys. B **21**, 1639 (1988).

[5] M. J. Brunger, J. L. Riley, R. E. Scholten, and P. J. O. Teubner, J. Phys. B **22**, 1431 (1989).

[6] J. Mitroy and I. E. McCarthy, J. Phys. B **22**, 641 (1989).

[7] I. E. McCarthy, K. Ratnavelu, and Y. Zhou, J. Phys. B **22**, 2597 (1989).

[8] G. D. Meneses, C. B. Pagan, and L. E. Machado, Phys. Rev. A **41**, 4610 (1990).

[9] For the unitarization procedure, see H. Saraph, M. J. Seaton, and J. Shemming, Philos. Trans. R. Soc. London **264**, 77 (1969); J. Davis, P. C. Kepple, and M. Blaha, J. Quant. Spectrosc. Radiat. Transfer **16**, 1043 (1976).

[10] FOMBT was introduced by G. Csanak, H. S. Taylor, and R. Yaris, Phys. Rev. A **3**, 1322 (1971). For FOMBT results on Ba target, see R. E. H. Clark, J. Abdallah, Jr., G. Csanak, and S. P. Kramer, Phys. Rev. A **40**, 2935 (1989).

[11] D. H. Madison and W. N. Shelton, Phys. Rev. A **7**, 499 (1973); D. H. Madison, J. Phys. B **12**, 3399 (1979).

[12] G. Csanak and D. C. Cartwright, Phys. Rev. A **34**, 93 (1986).

[13] R. E. H. Clark, J. Abdallah, Jr., G. Csanak, and S. P. Kramer, Phys. Rev. A **40**, 2935 (1989).

[14] R. E. H. Clark and J. Abdallah, Jr., in *Proceedings of the International Symposium on Correlation and Polarization in Electronic and Atomic Collisions,* NIST Special Publication 789, edited by P. A. Neill, K. H. Becker, and M. H. Kelley (U.S. Department of Commerce, National Bureau of Standards, Washington, DC, 1990), p. 22.

[15] J. Abdallah, Jr., R. E. H. Clark, and R. D. Cowan, Los Alamos National Laboratory Manual No. LA-11436-MI, 1988 (unpublished).

[16] R. D. Cowan, J. Opt. Soc. Am. **58**, 808 (1968).

[17] R. D. Cowan, J. Opt. Soc. Am. **58**, 924 (1968).

[18] R. D. Cowan and D. C. Griffin, J. Opt. Soc. Am. **66**, 1010 (1967).

[19] R. D. Cowan, *Theory of Atomic Spectra* (University of California Press, Berkeley, 1981).

[20] R. E. H. Clark, J. Abdallah, Jr., G. Csanak, J. B. Mann, and R. D. Cowan, Los Alamos National Laboratory Manual No. LA-11436-M, Vol. II, 1988 (unpublished).

[21] J. B. Mann, At. Data Nucl. Data Tables **29**, 407 (1983).

[22] H. E. Saraph, Comput. Phys. Commun. **3**, 256 (1972).
[23] R. E. H. Clark, Comput. Phys. Commun. **16**, 119 (1978).
[24] M. K. Inal and J. Dubau, J. Phys. B **20**, 4221 (1987).
[25] R. E. H. Clark, J. Abdallah, Jr., and S. P. Kramer, Los Alamos National Laboratory Manual No. LA-11436-M, Vol. III, 1988 (unpublished).
[26] A. A. Radzig and B. M. Smirnov, *Reference Data on Atoms, Molecules and Ions* (Springer-Verlag, New York, 1985).
[27] For the definition of λ and χ EICP's, see, e.g., Ref. [8].
[28] W. Williams and S. Trajmar, J. Phys. B **11**, 2021 (1978).
[29] I. S. Aleksakhin, I. P. Zapesochnyi, I. I. Garga, and V. P. Starodub, Opt. Spectrosc. **34**, 611 (1973).
[30] D. Leep and A. Gallagher, Phys. Rev. A **13**, 148 (1976).
[31] I. I. Fabrikant, J. Phys. B **13**, 603 (1980).